ATATÜRK ÜNİVERSİTESİ YAYINLARI
ATATURK UNIVERSITY PUBLICATIONS

Research Article *Araştırma Makalesi* DOI:10.5281/zenodo.14344088

Synthesis, FT-IR, DFT and *in silico* Antibacterial Activity Studies of Silver Nitrate Complex of Chlorzoxazone

Mustafa Tuğfan BİLKAN
Department of Biophysics, Tokat Gaziosmanpaşa University, Faculty of Medicine, Tokat, Türkiye
Zehra ÇAKIL
Tokat Gaziosmanpaşa University, Faculty of Medicine, Tokat, Türkiye
Elçin Özgür BÜYÜKATALAY
Department of Biophysics, Gazi University, Faculty of Medicine, Ankara, Türkiye

Chlorzoxazone Molekülünün Gümüş Nitrat Bileşiğinin Sentezlenmesi, FT-IR, DFT ve *in silico* Antibakteriyel Çalışmaları

Abstract

In this study, it was aimed to produce a new potential antibacterial agent using Chlorzoxazone and silver nitrate. Within the scope of the study, CZX.$AgNO_3$ structure was synthesized by chemical synthesis methods. The structure was experimentally characterized by FT-IR and elemental analysis. In addition, the optimized structure and vibration frequencies were obtained by the DFT method. After characterization, ADME and toxicity parameters of the new molecule were revealed using *in silico* methods. In order to determine the antibacterial effect of the molecule, molecular docking studies were performed on gram+ Staphylococcus aureus bacteria, and the data were compared with the frequently used antibiotic clindamycin. The results revealed the ADME, toxicity, and antibacterial effect of the new compound CZX.$AgNO_3$ is quite superior.

Keywords: Silver Nitrate, Chlorzoxazone, Molecular Spectroscopy, DFT, Molecular Docking, *in silico* ADMET prediction

Öz

Bu çalışmada, Klorzoksazon ve gümüş nitrat kullanılarak yeni bir potansiyel antibakteriyel ajan üretilmesi amaçlanmıştır. Çalışma kapsamında, CZX.$AgNO_3$ yapısı kimyasal sentez yöntemleri ile sentezlenmiştir. Oluşan yapı, FT-IR ve elementel analiz metotları ile deneysel olarak karakterize edilmiştir. Ayrıca, optimize edilmiş yapı ve titreşim frekansları DFT ile elde edilmiştir. Karakterizasyon işleminin ardından, molekülün ADME ve toksisite parametreleri *in silico* yöntemler kullanılarak belirlenmiştir. Molekülün antibakteriyel etkisini belirlemek amacıyla, gram+ Staphylococcus aureus bakterisi üzerinde moleküler kenetleme çalışmaları yapılmış ve veriler, sıklıkla kullanılan antibiyotik klindamisin ile karşılaştırılmıştır. Sonuçlar, yeni bileşik CZX.$AgNO_3$'ün ADME, toksisite ve antibakteriyel etkisinin oldukça üstün olduğunu ortaya koymuştur.

Anahtar Kelimeler: Gümüş Nitrat, Klorzoksazon, Moleküler Spektroskopi, DFT, Moleküler Yerleştirme, *in silico* ADMET tahmini

Corresponding Author/ Sorumlu Yazar:
Mustafa Tuğfan Bilkan
E-mail: mtbilkan@gmail.com

Received/ Geliş Tarihi 10.10.2024
Accepted/Kabul Tarihi 12.11.2024
Publication Date/ Yayın Tarihi 12.12.2024

Cite this article
Bilkan, M. T., Çakıl, Z. & Büyükatalay, E.Ö. (2024) Synthesis, FT-IR, DFT and in silico Antibacterial Activity Studies of Silver Nitrate Complex of Chlorzoxazone. *Journal of Anatolian Physics and Astronomy, 3*(2), 52-61.

Introduction

Chlorzoxazone (CZX) is an effective muscle relaxant to treat muscle spasms and the resulting pain and discomfort. Its relaxant effect on skeletal muscles was discovered in the late 1950s (Stewart et al., 1987). CZX shows this effect by blocking signals to the brain and causing muscle relaxation (Bai & Ma, 2020; Megalamani et al., 2023). It also has therapeutic effects on systemic mastocytosis, conjunctivitis, and ulcerative colitis (Tang et al.,2015). When a detailed examination is made, although many studies have been conducted on CZX recently (Bai & Ma, 2020; Skrejborg et al.,2020; Deng et al., 2020; Creteanu et al., 2024), to the best of our knowledge, there has yet to be a study on the silver metal complexes of CZX. This study aimed to produce and characterize the $AgNO_3$ metal compound of CZX. Silver nitrate is an odorless, white solid inorganic silver salt with the chemical formula $AgNO_3$. Although Albert Magnus first described it in the 13^{th} century, it was frequently used in the treatment of cuts and wounds due to its antiseptic properties in Roman and ancient Greek civilizations. Today, with this feature, it is used in the treatment of warts and also to prevent eye diseases caused by the Neisseria gonorrhoeae bacteria in newborn babies (Bilkan et al., 2016). In addition to its antibacterial properties, silver nitrate injection therapy has a long history of use in urology (Sekito et al., 2022). Due to its medical and pharmacological importance, the production of new molecular structures containing silver nitrate has gained significant importance in the last ten years. In this context, in 2023, Aveledo et al. conducted studies on silver nitrate using the Calvet calorimeter (Aveledo et al., 2023). Gutmańska et al. obtained new silver compounds containing 1,4-dicyanobenzene and 3-cyanopyridine (Gutmańska et al., 2022). Pereira et al. conducted toxicity studies on silver nitrate and other silver materials (Pereira et al., 2023). Eady et al. studied Salmonella detection using SERS spectroscopy on silver nitrate nanoparticles (Eady et al., 2023). Recently, Karan and Erenler synthesized silver nanoparticles using antioxidant-effective potato varieties (Karan & Erenler, 2024). In this study, it was aimed to produce a new compound containing $AgNO_3$ and CZX due to their stated medical and pharmacological importance. CZX.$AgNO_3$ structure was produced using CZX and $AgNO_3$. The structure of the compound was characterized by FT-IR and molecular modeling. Pharmacokinetic parameters and toxicity profiles of the compound were determined. In addition, in order to determine the antibacterial activity, binding conditions of Staphylococcus aureus bacteria with tyrosyl-tRNA synthetase (PDB ID: 1JIJ) receptor were revealed. The obtained results were compared with the results of the well-known antibiotic clindamycin, and it was found that the newly produced compound has excellent antibacterial agent potential.

Experimental and Computational Procedures

CZX and $AgNO_3$ were supplied by Sigma-Aldrich for the production of the compound. Since it has poor water solubility, two mmol CZX was dissolved in 5 ml ether. One mmol $AgNO_3$ was dissolved in 3 ml pure water. Both solutions were stirred at room temperature for 10 min and added to each other. The final mixture was stirred at 300 K for 5 min, and the precipitate formed was collected using filter paper. The collected material was dried in a sterile oven and stored at +4 ˚C for analysis. CHNS analyses were performed with varioMICRO CHNS analyzer. FT-IR recordings were performed with Bruker FRA 106/S Spectrometer. In the theoretical studies section, the Gaussview program was used to draw all three-dimensional compounds (Dennington et al., 2008). The drawings were optimized with Gaussian (Frisch et al., 2010), and physical, chemical, spectroscopic, and electronic properties were determined. Potential Energy Distributions for each vibration mode were obtained with the VEDA4 program (Jamróz, 2004). Protox 3.0 to predict the toxicities of the compounds (Banerjee et al., 2024) was used. The PreADMET webserver was utilized to determine the ADME parameters of the compounds (Seul, 2004). Molegro Virtual Docker program was used (Bitencourt et al., 2019) in docking analyses. In the calculations, DFT/6-311++G(d,p) was used for CZX, and LanL2DZ was used for CZX.$AgNO_3$. Corrections were made by multiplying the vibration frequencies with scale factors 0.9982 for CZX and 0.9668 for silver nitrate complexes. CHN analyses results for CZX.$AgNO_3$: found H(1.47%), C(32.89%), N(1.63%); calc H(1.58%), C(33.04%), N(1.58%).

Results and Discussion

Three-Dimensional Structure and Geometrical Parameters

The stable geometry of a molecular structure plays a fundamental role in determining many physical and chemical parameters of the molecule. The smallest changes in structural parameters directly affect characteristic properties, especially vibration frequencies. Therefore, the first step before working on molecular systems is to obtain a three-dimensional optimized structure. For this purpose, in this study, the three-dimensional structures of CZX and CZX.$AgNO_3$ molecules were optimized with DFT, and the results are shown in Figure 1.

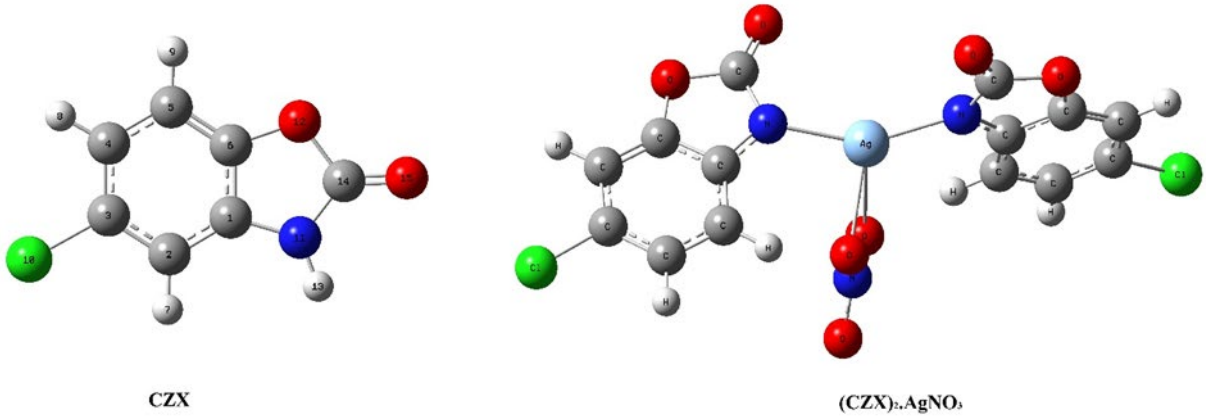

Figure 1. Optimized molecular structures of CZX and CZX.$AgNO_3$

As seen in Figure 1, the silver atom is bonded with two CZX molecules. As expected, chemical bonding occurred between the nitrogen atoms of the CZX molecule and the silver atom. The calculated parameters of the three-dimensional geometry and the experimental parameters of the CZX molecule are shown in Table 1 (Selected).

Table 1. Selected important geometric parameters of the structures (Å and ˚).

Parameters	CZX		CZX.$AgNO_3$		CZX		CZX.$AgNO_3$
	Calc.	Exp.*	Calc.	Parameters	Calc.	Exp.*	Calc.
1C-2C	1.385	1.393	1.421	6C-12O	1.376	1.391	1.386
1C-11N	1.390	1.387	1.372	3C-10Cl	1.758	1.738	1.799
11N-14C	1.384	1.352	1.415	5C-6C	1.377	1.380	1.385
14C-15O	1.196	1.204	1.225	12N-15Ag	-	-	2.160
14C-12O	1.392	1.378	1.465	15Ag-30O	-	2.384	2.316
1C-11N-14C	110.60	110.74	107.74	15Ag-31O	-	-	2.799
1C-6C-12O	109.61	108.44	108.92	2C-12N-15Ag	-	-	129.92
6C-12O-14C	108.27	107.83	105.78	13C-12N-15Ag	-	-	117.83
12O-14C-11N	106.34	107.54	108.49	12N-15Ag-30O	-	-	91.39
12O-14C-15O	124.23	122.04	121.94	12N-15Ag-31O	-	-	104.78
15O-14C-11N	129.43	130.55	129.57	30O-32N-31O	-	-	116.82

*Data were taken from Ref (Bilkan et al., 2016)

As seen in the table, all geometric parameters calculated with DFT are in good agreement with the experimental data taken from the literature (İde & Topaç, 1997). Especially for CZX, the parameters between the atoms in the aromatic ring were calculated with minor deviations. While the length between 1C-2C atoms was 1.393 Å experimentally, it was calculated as 1.385 Å with DFT. There is only a 0.008 Å difference between the two. Another parameter, 1C-11N bond length, was calculated as 1.390 Å, and its experimental value is 1.387 Å. The deviation is 0.003 Å. Similar results are seen for all other bond lengths. The highest deviation is between 0.02 Å and 3C-10Cl atoms, well below the acceptable limit of 0.1 Å. The N-Ag bond length is calculated as 2.16 Å. It is known from the literature that the experimental value is 2.39 Å (Bilkan et al., 2016). In this case, it has been shown that the optimized structure obtained with DFT approaches the experimental values very well. The agreement between the experimental and calculated parameters is also seen in the bond angles. There are deviations of 1-2˚ in the bond angles between atoms.

Vibrational Modes Analyses

Fourier Transform Infrared Spectroscopy (FT-IR) is a very useful method that allows the characterization of molecular structures by determining the vibration frequencies and intensities of a molecular structure. The method is frequently used in obtaining the structures of biologically active agents. In this study, the FT-IR spectrum for the CZX.$AgNO_3$ compound produced was recorded with ATR and is given in Figure 2. Experimental IR vibration modes for CZX were taken from the literature (Gnanasambandan et al., 2014).

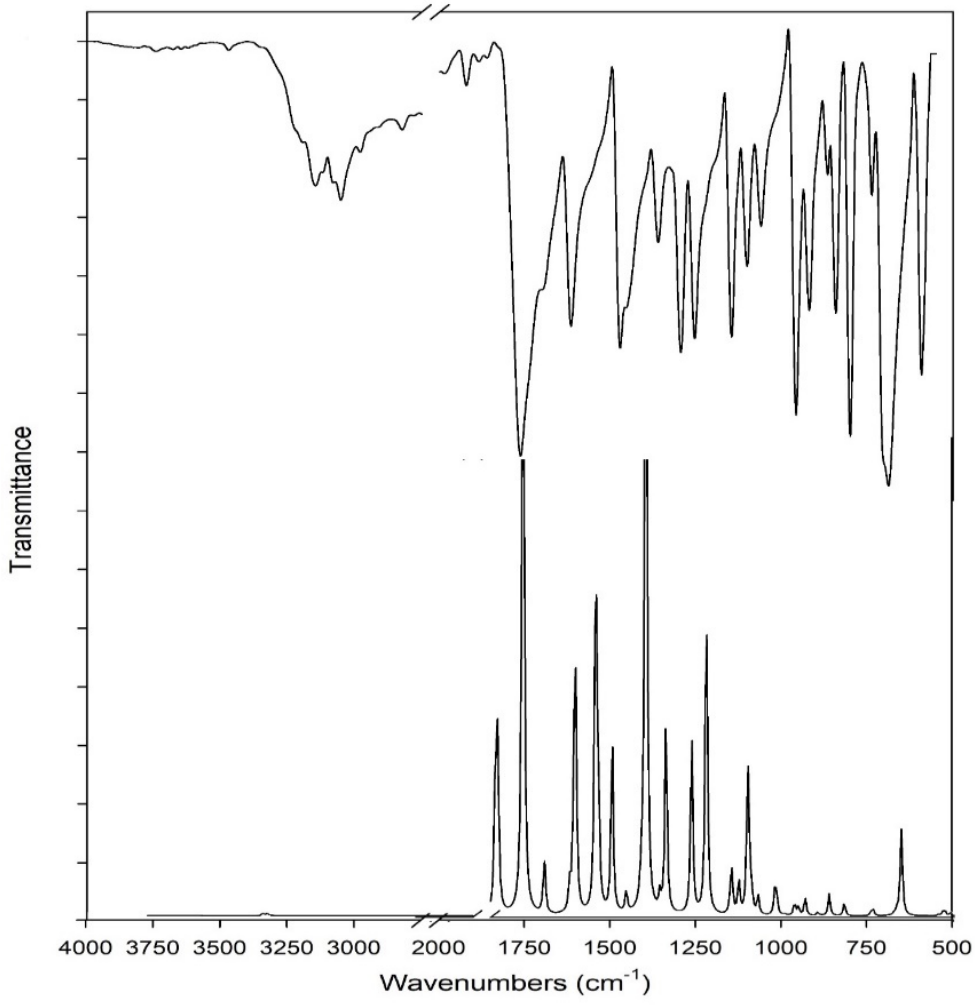

Figure 2. Calculated and recorded mid-IR spectra of CZX.AgNO3

When Figure 2 is examined, it is seen that the recorded and calculated IR modes for the compound are in good agreement with each other. The number of vibrational modes of a compound with N atoms is given by 3N-6. CZX has fifteen atoms and thus thirty-nine fundamental vibrational modes, while CZX.$AgNO_3$ has 33 atoms and 93 fundamental vibrational modes. Some important vibrational modes calculated by DFT, together with those obtained experimentally, are given in Table 2. Calculations were performed with the basis set 6-311++G(d,p) for CZX and the basis set LANL2DZ for $AgNO_3$. The calculated modes were scaled with the scaling factors 0.9668 and 0.9612 to obtain better agreement with the experimental ones.

Table 2. The calculated and experimental selected vibrational modes of CZX and CZX.$AgNO_3$

Mode	CZX			CZX.$AgNO_3$			PED (%)
	Exp.	Calculated		Exp.	Calculated		
	IR*	Freq.	IR	IR	Freq.	I_{IR}	
32	592s	577	1.54	571m	530	0.97	δ_{CCC} (11)
38	-	-	-	593w	609	0.03	δ_{ONO} (76)+V_{ON}(13)
39	-	-	-	596w	618	0.43	δ_{ONO} (85)
40	639m	591	0.18	622w	658	1.67	V_{ClC}(16)+δ_{CCC} (14)+V_{CC}(10)
42	-	-	-	668w	679	0.22	δ_{CNAg} (15)+δ_{CCC} (11)+V_{CC}(10)
46	751w	735	0.84	705m	695	0.96	Γ_{ONOC}(64)
50	-	-	-	719sh	758	2.96	δ_{OCC}(24)+δ_{CCC} (24)+δ_{CNAg} (10)
51	842s	837	2.37	802m	813	2.47	Γ_{HCCN}(46)+Γ_{HCCC}(44)
54	920s	900	5.77	849w	848	14.04	δ_{CCC} (24)+V_{OC}(22)+δ_{CNAg} (10)
56	868w	852	0.08	867w	877	2.37	Γ_{HCCC}(78)
59	-	-	-	914m	904	2.03	V_{ON}(93)
63	959vs	920	0.06	950s	984	19.66	V_{NC}(54)
65	1061m	1054	2.38	1029w	1031	4.76	V_{CC}(35)+ δ_{HCC} (17)+V_{ClC}(13)
66	-	-	-	1106w	1115	26.47	V_{ON}(79)+ δ_{ONO}(14)
68	1147s	1132	2.42	1149m	1136	1.18	δ_{HCC}(48)+V_{CC}(14)
70	1102m	1080	2.14	1254w	1196	3.09	V_{OC}(38)
73	1230w	1230	0.59	1257m	1292	19.21	V_{NC}(32)+ δ_{HCC} (15)+V_{CC}(12)
75	-	-	-	-	1337	15.10	V_{ON}(83)
76	1295s	1269	3.84	1362w	1346	48.89	V_{CC}(24)
79	1456m	1457	1.05	1453sh	1417	16.65	δ_{HCC}(39)+δ_{CCC}(10)
81	-	1352	1.31	1482s	1432	2.37	V_{CC}(36)+δ_{HCC}(26)
84	1616s	1621	2.97	1622m	1584	100.0	V_{CC}(51)
86	1764vs	1843	100.0	1778vs	1667	21.38	V_{OC}(81)
93	3082w	3149	0.04	3118w	3163	0.28	V_{CH}(98)

C-H stretching vibration is observed in the range of 3100-3200 cm^{-1}. C-H stretching vibrations were obtained at 3149 and 3163 cm^{-1} wave numbers for the compounds examined in this study. Carboxyl-containing molecules generally show intense bands around 1700-1800 cm^{-1} due to the intense observation of C-O vibrations. Since CZX contains a carboxyl group, the most intense vibration mode was calculated at 1843 cm^{-1} and was observed experimentally at 1764 cm^{-1}. The reason for the difference is that the calculations were obtained for a single molecule in the gas phase, while the experimental results were recorded for n mol of molecules. The modes calculated at 609, 618, and 679 cm^{-1} for CZX.$AgNO_3$ were not observed in CZX. These modes are due to the internal vibrations of $AgNO_3$ and ligand-metal bonds. These results and CHN analyses

prove that the structure produced from chemical synthesis is compatible with the theoretically modeled 2-1 bonded CZX.$AgNO_3$ structure.

Pharmacokinetic Properties and Toxicity Profile of CZX.AgNO3

The absorption, distribution, metabolism and elimination (ADME) processes of a drug are called pharmacokinetic parameters and provide crucial preliminary information, especially in determining the effectiveness of pharmacological agents in the body. Biological activity can be estimated with high accuracy by examining the functional groups of compounds and comparing them with experienced drugs. In this study, ADME parameters for the CZX.$AgNO_3$ compound were obtained by *in silico* methods and compared with those of clindamycin, one of the essential antibiotics. The results are shown in Table 3.

Table 3. Some important in silico ADME parameters of clindamycin and CZX.$AgNO_3$

ID	clindamycin	CZX.$AgNO_3$
BBB (C_{brain}/C_{blood})	0.09	1.08
Caco-2 (nm/sec)	20.43	33.47
HIA (%)	84.30	100.00
MDCK (nm/sec)	0.55	0.35
Plasma Protein Binding (%)	33.65	78.77
Pure water solubility mg/L	700.3	2084.4
Skin Permeability (cm/hour)	-4.27	-3.07

BBB, one of the parameters in the table, represents the blood-brain barrier permeability. It is known as the ratio of the intracranial concentration of a drug to its concentration in plasma. A value greater than two indicates that drugs may significantly affect the central nervous system (CNS). As can be seen from the table, both compounds have a weak effect on the CNS. The Caco-2 and MDCK parameters represent the intestinal epithelial barrier and kidney cell line, respectively, and represent the number of molecules absorbed per second in nanomoles. While the Caco-2 absorption of clindamycin and CZX.$AgNO_3$ is at a medium level; the MDCK absorption is low. Another important ADME parameter is the HIA value. This parameter, known as Human Intestinal Absorption, gives the absorption percentage from the small intestine. Accordingly, while clindamycin is absorbed by 84.30%, CZX.AgNO3 is absorbed by 100% from the small intestine. Plasma protein binding rate gives the binding rates of drugs to proteins known as plasma proteins, such as albumin, fibrinogen, and globulin. The higher the binding rate, the lower the drug's effectiveness. However, a binding rate below 90% is considered sufficient for the effectiveness of drugs. In this context, it can be said that the PPB rate of CZX.$AgNO_3$ is sufficient. In Table 4, *in silico* predicted toxicity profiles of the compounds were given.

The LD50 value (Lethal Dose 50) is the amount of toxic substance that causes the survival of a population to decrease to 50%. As the LD50 value increases, the toxicity decreases. Therefore, it is seen that CZX.$AgNO_3$ has lower toxicity compared to clindamycin. In addition, the toxicity class was determined as 4 for clindamycin, while it was found as 5 for CZX.$AgNO_3$. However, there are cases where the toxic effects of both compounds are active and inactive. For example, clindamycin has toxic effects on the immune system, while CZX.$AgNO_3$ has toxic effects on the liver. This is one of the important situations that should be considered in the research of the compound as a drug.

Table 4. The in silico predicted toxicity parameters of clindamycin and CZX.$AgNO_3$ compounds

ID	clindamycin		CZX.$AgNO_3$	
Predicted LD_{50} (mg/kg)	1095		2161	
Predicted Toxicity Class	4	harmful if swallowed	5	May be harmful if swallowed
	Probability	**Prediction**	**Probability**	**Prediction**
Hepatotoxicity	0.65	Inactive	0.51	**Active**
Immunotoxicity	0.84	**Active**	0.95	Inactive
Cytotoxicity	0.73	Inactive	0.69	Inactive
Carcinogenicity	0.63	Inactive	0.56	Inactive
Mutagenicity	0.73	Inactive	0.55	Inactive
Neurotoxicity	0.81	Inactive	0.64	**Active**
Nephrotoxicity	0.51	**Active**	0.58	**Active**
Respiratory toxicity	0.78	**Active**	0.51	**Active**
Cardiotoxicity	0.73	Inactive	0.62	Inactive

Investigation of Antibacterial Activity

Molecular docking is, in general terms, a macromolecular simulation method used to determine the interaction of a molecule with a target receptor. It is generally used to examine the therapeutic effects of a drug on a disease. After the interaction, a binding score is obtained and this score is directly proportional to the binding efficiency. This binding is mostly based on the inhibition of the protein that is the causative agent of the disease. The degenerations caused by the binding in the structure of the protein stop the proteins from performing their specialized function, and thus, the therapeutic effect occurs. In this study, the antibacterial effect was investigated by comparing the binding affinities of CZX.$AgNO_3$ and clindamycin (as positive control) with the tyrosyl-tRNA synthetase (PDB ID: 1JIJ) receptor enzyme of Staphylococcus aureus bacteria. Staphylococcus aureus (S. aureus) causes some serious infections, such as endocarditis, and has significant lethal effects. The binding scores and other relevant parameters obtained as a result of docking operations are given in Table 5.

As seen in the table, CZX.$AgNO_3$ performed eight hydrogen bonds with the target receptor. In these bindings, the molecule acted as a hydrogen acceptor and interacted with the amino acids Gly193, Gln196, Gln174, Tyr170 (two bonds), and Asp40 (three bonds) of the protein. The MolDock score of the binding was obtained as -152.123, and a significant portion of the total binding energy originated from steric hindrance (PLP) energy. The binding score for clindamycin was obtained as -127.065. This result confirms that the CZX.$AgNO_3$ molecule binds to the relevant receptor better than the positive control clindamycin. The bindings for both molecular structures are given in Figure 3.

Table 5. The interaction parameters between clindamycin, CZX.AgNO3 and the target protein

Parameters	clindamycin	CZX.$AgNO_3$
MolDock Score	-127.065	-152.123
Rerank Score	-112.459	-116.705
Hydrogen Bonding energy (kcal/mol)	-3.44782	-7.256
Steric Hindrance Energy (PLP)	-141.458	-136.016
Steric Hindrance Energy (LJ12-6)	-45.523	-45.835
Electrostatic Interaction Energy Short range	-	-
Electrostatic Interaction Energy Long range	-	-
Amino acid-drug bonding (bond length: Å, bond energy: kcal/mol)	Tyr170(O)-ligand(O-H) b.l.:2.81-b.e.:-2.50 Asp40(O)-ligand(O-H) b.l.:2.46-b.e.:-0.74 Thr75(O-H)-ligand(O) b.l.:3.00-b.e.:-2.50 Asp40(O)-ligand(O-H) b.l.:3.17-b.e.:-2.16	Gly193(N-H)-ligand(O) b.l.:2.76-b.e.:-2.50 Gln196(N-H)-ligand(N) b.l.:3.49-b.e.:-0.53 Gln174(N-H)-ligand(O) b.l.:2.89-b.e.:-2.50 Tyr170(O-H)-ligand(O) b.l.:2.76-b.e.:-2.50 Tyr170(O-H)-ligand(O) b.l.:2.83-b.e.:-1.34 Asp40(O-H)-ligand(O) b.l.:3.12-b.e.:-1.92 Asp40(O-H)-ligand(O) b.l.:2.97-b.e.:-0.84 Asp40(N-H)-ligand(N) b.l.:3.46-b.e.:-0.68

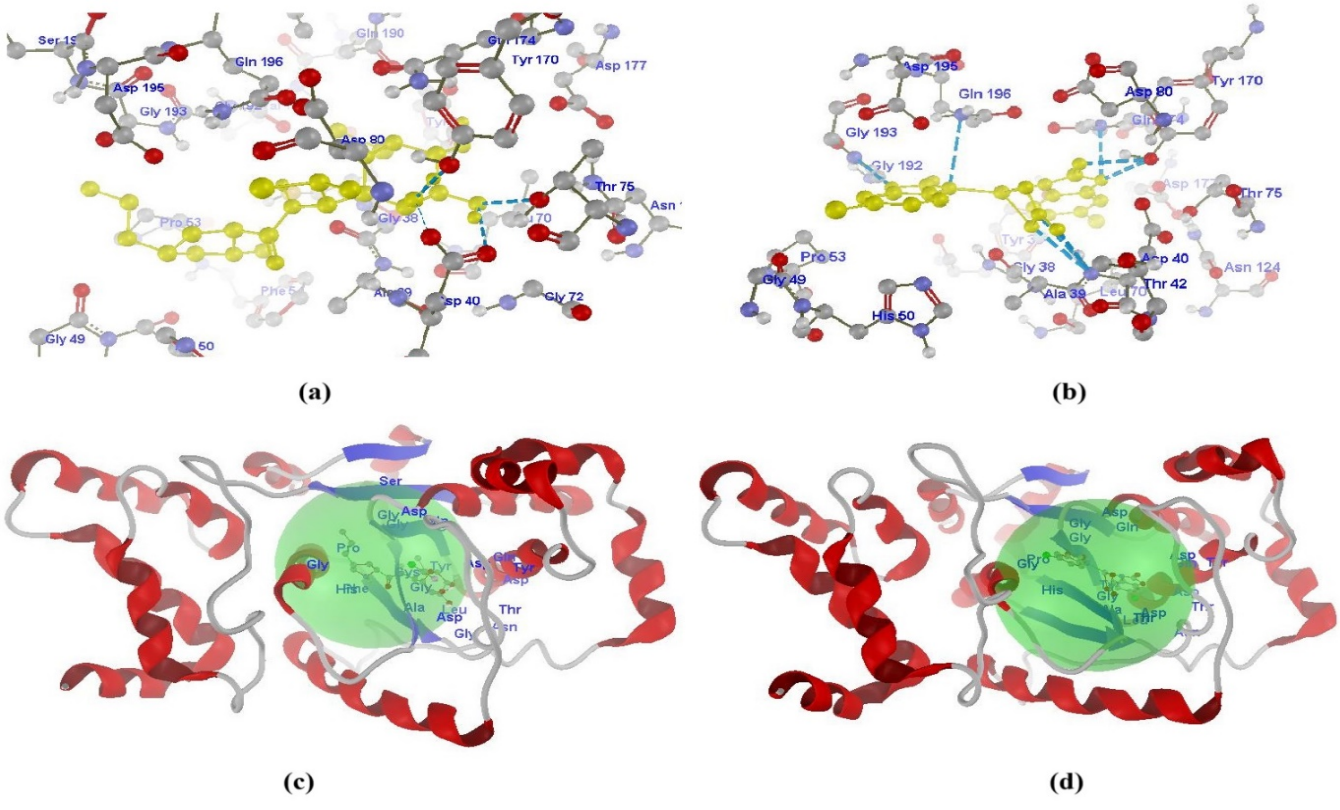

Figure 3. The three-dimensional molecular docking structures and interaction parameters of 1JIJ protein with clindamycin and CZX.$AgNO_3$

Figures 3a and 3b represent the binding positions of the compounds to amino acids of the target receptor on a near scale. Figures 3c and 3d show that both compounds (clindamycin and CZX.$AgNO_3$) bind to the same active sites of the target protein—however, CZX.$AgNO_3$ has a superior binding score (-25.058 kcal/mol) than clindamycin. These results support that the potential antibacterial agent may exhibit similar binding properties to clindamycin and, thus, therapeutic effects.

Conclusion

In this study, a new potential antibacterial agent CZX.$AgNO_3$ was synthesized. The synthesized structure was characterized using experimental and theoretical methods. ADME and toxicity profiles of the molecule were determined in silico. In addition, the antibacterial activity of the molecule was carried out by molecular docking analyses. The obtained results were compared with the positive control group clindamycin and the following results were obtained:

- The geometrical structure studies show that the optimized structure obtained with DFT approaches the experimental values very well.
- CHN analyses reveal that the structure produced from chemical synthesis is compatible with the theoretically modeled 2-1 bonded CZX.$AgNO_3$ structure.
- ADME results show that CZX.$AgNO_3$ has a weak effect on the CNS. Moreover, CZX.$AgNO_3$ is absorbed 100% by the human intestinal system.
- *in silico* studies reveal that new compound CZX.$AgNO_3$ has lower toxicity compared to conventional drug clindamycin.
- Molecular docking results support the CZX.$AgNO_3$ may has antibacterial effect because it exhibits similar binding properties to clindamycin.

Peer-review: *Externally peer-reviewed.*
Author Contributions: *Concept–MTB, EÖB; Design- MTB, ZÇ, EÖB; Supervision- MTB; Resources- MTB, ZÇ; Data Collection and/or Processing- MTB, ZÇ; Analysis and/or Interpretation- MTB, EÖB; Literature Search- MTB, ZÇ; Writing Manuscript- MTB, ZÇ, EÖB; Critical Review- MTB, ZÇ, EÖB Other- MTB, ZÇ, EÖB*
Conflict of Interest: *The authors have no conflicts of interest to declare.*
Financial Disclosure: *The authors declared that this study has received no financial support.*

Hakem Değerlendirmesi: *Dış bağımsız.*
Yazar Katkıları: *Fikir-MTB, EÖB; Tasarım- MTB, ZÇ, EÖB; Denetleme- MTB; Kaynaklar-MTB, ZÇ; Veri Toplanması ve/veya İşlemesi MTB, ZÇ; Analiz ve/ veya Yorum- MTB EÖB; Literatür Taraması-MTB, ZÇ; Yazıyı Yazan- MTB, ZÇ, EÖB;; Eleştirel İnceleme- MTB, ZÇ, EÖB*
Çıkar Çatışması: *Yazarlar, çıkar çatışması olmadığını beyan etmiştir.*
Finansal Destek: *Yazarlar, bu çalışma için finansal destek almadığını beyan etmiştir.*

References

Aveledo, R., Aveledo, A., Lago, N., Mato, M. M., & Legido, J. L. (2023). Antibacterial activity of silver nitrate on Pseudomonas aeruginosa bacteria using Calvet calorimetry. *Journal of Thermal Analysis and Calorimetry*, 148(4), 1639-1646.

Bai, Y., & Ma, X. (2020). Chlorzoxazone exhibits neuroprotection against Alzheimer's disease by attenuating neuroinflammation and neurodegeneration in vitro and in vivo. *International Immunopharmacology*, 88, 106790.

Banerjee, P., Kemmler, E., Dunkel, M., & Preissner, R. (2024). ProTox 3.0: a webserver for the prediction of toxicity of chemicals. *Nucleic Acids Research*, gkae303.

Bilkan, M. T., Yurdakul, Ş., Demircioğlu, Z., & Büyükgüngör, O. (2016). Crystal structure, FT-IR, FT-Raman and DFT studies on a novel compound [C10H9N3] 4AgNO3. *Journal of Organometallic Chemistry*, 805, 108-116.

Bitencourt-Ferreira, G., & de Azevedo, W. F. (2019). Molegro virtual docker for docking. *Docking screens for drug discovery*, 149-167.

Creteanu, A., Lisa, G., Vasile, C., Popescu, M. C., Pamfil, D., Lungu, C. N., ... & Tantaru, G. (2024). New Hydrophilic Matrix Tablets for the Controlled Released of Chlorzoxazone. *International Journal of Molecular Sciences*, 25(10), 5137.

Deng, L., Li, H., Su, X., Zhang, Y., Xu, H., Fan, L., ... & Zhao, R. C. (2020). Chlorzoxazone, a small molecule drug, augments immunosuppressive capacity of mesenchymal stem cells via modulation of FOXO3 phosphorylation. *Cell Death & Disease*, 11(3), 158.

Dennington, R. D., Keith, T. A., & Millam, J. M. (2008). GaussView 5.0, Gaussian. Inc., Wallingford, 20.

Eady, M., Setia, G., Park, B., Wang, B., & Sundaram, J. (2023). Biopolymer encapsulated silver nitrate nanoparticle substrates with surface-enhanced Raman spectroscopy (SERS) for Salmonella detection from chicken rinse. *International Journal of Food Microbiology*, 391, 110158.

Frisch, M. J., Trucks, G. W., Schlegel, H. B., Scuseria, G. E., Robb, M. A., Cheeseman, J. R., ... & Cioslowski, J. (2010). Gaussian 09 Revision B. 01 M., and Revision A. 02 SMP J. Gaussian, Inc., Wallingford, CT.

Gnanasambandan, T., Gunasekaran, S., & Seshadri, S. (2014). FT-IR, FT-Raman, UV–Vis spectral and normal coordinate analysis of chlorzoxazone. *Journal of Molecular Structure*, 1061, 124-133.

Gutmańska, K., Ciborska, A., Hnatejko, Z., & Dołęga, A. (2022). Nitrate and nitrite silver complexes with weakly coordinating nitriles. *Polyhedron*, 220, 115831.

İde, S., & Topaç, A. (1997). Tautomeric investigations and crystal structure analysis of chlorzoxazone. *Journal of chemical crystallography*, 27, 303-306.

Jamróz, M. H., (2004). Vibrational Energy Distribution Analysis. VEDA 4, Warsaw.

Karan, Y. B., & Erenler, R. (2024). Synthesis of Silver Nanoparticles Using Potato Cultivars with Their Antioxidant Activity. *Communications in Soil Science and Plant Analysis*, 1-9.

Megalamani, M. B., Patil, Y. N., & Nandibewoor, S. T. (2023). YSZ/MoS2 modified carbon based sensor for the determination of muscle relaxant agent chlorzoxazone: A novel electroanalytical strategy. *Inorganic Chemistry Communications*, 155, 111074.

Pereira, S. P., Boyle, D., Nogueira, A. J., & Handy, R. D. (2023). Comparison of toxicity of silver nanomaterials and silver nitrate on developing zebrafish embryos: Bioavailability, osmoregulatory and oxidative stress. *Chemosphere*, 139236.

Sekito, T., Sadahira, T., Watanabe, T., Maruyama, Y., Watanabe, T., Iwata, T., ... & Watanabe, M. (2022). Medical uses for silver nitrate in the urinary tract. *World Academy of Sciences Journal*, 4(1), 1-6.

Seul, S. C. (2004) Bioinformatics and Molecular Design Research Center;. PreADMET program.

Stewart, J. T., & Janicki, C. A. (1987). Chlorzoxazone. In Analytical profiles of drug substances (Vol. 16, pp. 119-144). Academic Press.

Skrejborg, P., Petersen, K. K., Beck, J., Ulrich, M., Simonsen, O., Nielsen, P. T., ... & Laursen, M. (2020). Investigating the effect of perioperative chlorzoxazone on acute postoperative pain after total hip and knee replacement surgery. *The Clinical Journal of Pain*, 36(5), 352-358.

Tang, P., Li, S., Wang, L., Yang, H., Yan, J., & Li, H. (2015). Inclusion complexes of chlorzoxazone with β- and hydroxypropyl-β-cyclodextrin: characterization, dissolution, and cytotoxicity. *Carbohydrate polymers*, 131, 297-305.